ОБЪЕДИНЕННЫЙ
ИНСТИТУТ
ЯДЕРНЫХ
ИССЛЕДОВАНИЙ
ДУБНА

E1 - 10838

INELASTIC INTERACTIONS OF ^{12}C NUCLEI WITH EMULSION NUCLEI AT 50 GeV/c

1977

M.I.Adamovich,[1] V.A.Bakaev,[2] B.P.Bannik, V.G.Bogdanov,[3] S.D.Bogdanov,[2] R.A.Bondarenko,[4] G.M.Chernov,[6] M.M.Chernyavsky,[1] A.El-Naghy, B.V.Gubinsky,[2] K.G.Gulamov,[6] U.G.Gulamov,[4] M.Haiduc,[7] M.Karabova,[5] S.P.Kharlamov,[1] V.G.Larionova,[1] A.Marin,[7] U.Michalschak,[5] S.Nasyrov,[4] D.Neagu,[7] V.I.Ostroumov,[2] N.A.Perfilov,[3] G.D.Pestova, V.A.Plyushchev,[3] J.A.Salomov, G.S.Shabratova, M.Sherif, E.Siles,[5] S.I.Solovieva,[3] L.M.Svechnikova,[6] E.Skrzypczak,[8] J.Szonert,[8] K.D.Tolstov, S.Vokal[5]

---

[1] *P.N.Lebedev Physical Institute, USSR Academy of Sciences, Moscow.*
[2] *M.I.Kalinin Polytechnical Institute, Leningrad.*
[3] *V.G.Khlopin Radium Institute, Leningrad.*
[4] *Institute of Nuclear Physics, Uzbek SSR Academy of Sciences, Tashkent.*
[5] *P.I.Shafarik University Kosice, Czechoslovakia.*
[6] *S.V.Starodubtsev Physical Technical Institute, Uzbek SSR Academy of Sciences, Tashkent.*
[7] *Central Institute of Physics, Bucharest, Romaina.*
[8] *University of Warsaw, Poland.*

E1 - 10838

INELASTIC INTERACTIONS OF ^{12}C NUCLEI WITH EMULSION NUCLEI AT 50 GeV/c

Submitted to International Conference on High Energy Physics and Nuclear Structure (Zurich, 1977) and International Conference on Cosmic Ray Physics (Plovdiv, 1977).

Адамович М.И. и др. **E1 - 10838**

Неупругие взаимодействия ядер ^{12}C с импульсом 50 ГэВ/с с ядрами фотоэмульсии

Исследовались неупругие взаимодействия ядер углерода с импульсом 50 ГэВ/с с ядрами фотоэмульсии. Получены распределения по множественности и угловые распределения вторичных заряженных частиц. Средние множественности, рассчитанные на один взаимодействующий нуклон ядра углерода, совпадают с аналогичными данными для взаимодействий дейтонов и α-частиц с ядрами фотоэмульсии.

В 90% случаев неупругих взаимодействий наблюдаются заряженные фрагменты ядра углерода. Угловые распределения фрагментов ядра мишени слабо зависят от атомного номера налетающего ядра. С частотой около 2% от числа неупругих взаимодействий наблюдается процесс диссоциации ядра углерода на три α-частицы.

Работа выполнена в Лаборатории высоких энергий ОИЯИ.

Препринт Объединенного института ядерных исследований. Дубна 1977

Adamovich M.I. et al. **E1 - 10838**

Inelastic Interactions of ^{12}C Nuclei with Emulsion Nuclei at 50 GeV/c

Inelastic interactions induced by ^{12}C relativistic nuclei, accelerated by the JINR synchrophasotron in Dubna, were studied. Multiplicity and angular distributions of charged secondaries were analysed. The average multiplicities, per one incident nucleon, are close to those for ^{2}H and ^{4}He primaries at the same momentum per nucleon.

The angular distributions of the target fragments (black and grey tracks) are very weakly dependent on the mass number of the incident nucleus. In 90% of ^{12}C inelastic interactions, fragments of the projectile nucleus were observed. About 2% of inelastic ^{12}C interactions correspond to the process of dissociation of the projectile nucleus into three helium nuclei; in most cases it can be interpreted as a two-stage process, involving an intermediate ^{8}Be nucleus.

Preprint of the Joint Institute for Nuclear Research. Dubna 1977

I. INTRODUCTION

The interest in high-energy nucleus collisions with nuclei has greatly increased during a few recent years. This is due to the possibility of appearance of collective nuclear matter at high density and the validity of scaling in the case of collisions of compound systems /1/. The aim of the present work is to obtain basic experimental characteristics of the multiparticle production process in inelastic interactions of ^{12}C ($p \simeq 4.2$ GeV/nucleon) with emulsion nuclei.

II. EXPERIMENTAL PROCEDURE

Stacks of Br-2 nuclear emulsion were exposed to a 50 GeV/c carbon beam at the High Energy Laboratory of JINR. The intensity of the exposure was 2×10^4 particles/cm^2. Light nuclei with the charge $Z \leq 5$ constituting a negligible fraction of the beam particles were visually identified and rejected.

Along the track double-scanning, fast in the forward and slow in the backward direction, was carried out. The total length of the scanned tracks equals 337.9 m; 2468 inelastic interactions were picked up. The one-prong events, with an emission angle of secondary particle $\theta<3°$ and no visible tracks from excitation or disintegration of incident particle and/or target-nucleus, were excluded as due to elastic scattering. For a further analysis 852 inelastic interactions were used.

In table I the obtained value of the mean free path for inelastic ^{12}C–A interactions is presented as well as the data for dA and αA collisions at the same momentum per nucleon [2,3].

Table I

Average mean free path values for inelastic interactions in the nuclear emulsion at a momentum of 4.2 GeV/c per nucleon.

Target nucleus	λ exp. (cm)	λ theor. (cm)	λ exp [5]
^{2}H	26.9 ± 0.6	24.1	
^{4}He	19.5 ± 0.3	19.9	21.8 ± 0.7
^{12}C	13.7 ± 0.3	13.8	12.8 ± 0.9 13.8 ± 0.5

The table presents also the values ($\lambda_{theor.}$) obtained on the basis of the formula

$$\sigma = \pi r_0^2 (A_T^{1/3} + A_B^{1/3} - b)^2 ,$$

where A_T and A_B are the mass numbers of target and beam nuclei and $r_0 = 1.23$ fm, $b = 1.56 - 0.2 (A_T^{1/3} + A_B^{1/3})$ [4]. In the last column of the table are the experimental values of λ for the ^{4}He and ^{12}C interactions (at 2.1 GeV/c/nucleon) with the emulsion nuclei obtained in /5/.

The charged secondary particles were divided into the following groups:

1. Slow (kinetic energy for proton $T_p \leq$ ≤ 400 MeV), heavily ionizing (h) particles, h particles with a dip angle of $\alpha \leq 30°$ were further divided into black (b) (with $T_p < 26$ MeV) and grey (g) tracks ($T_p > 25$ MeV). In order to take into account all the black and grey tracks (including those with $\alpha > 30°$) in the distributions, a geometrical correction or weighting factor K was used for b and g tracks emitted at large angles $\theta > 30°$.

$$K = \frac{\pi/2}{\arcsin \frac{\sin 30°}{\sin\theta}} .$$

2. Relativistic particles of relative ionization $g/g_0 < 1.4$ (corresponding proton energy $T_p > 400$ MeV), where g_0 is the ionization at the "plateau" in our emulsion stacks

2a) with an emission angle of $\theta > 3°$

2b) with an emission angle of $\theta \leq 3°$

3. Double-charged fragments of the incident nucleus defined as tracks with $g/g_0 \approx 4$ (with no change of ionization when followed up to a distance of at least 2 cm from the interaction) and with an emission angle of $\theta < 3°$.

4. Multicharged ($Z \geq 3$) fragments of the incident nucleus defined as tracks with $g/g_0 > 6$ (with no change of ionization when followed up to a distance of ~1 cm from the interaction) and with an emission angle of $\theta \leq 3°$

The charge of relativistic fragments of the incident nuclei was determined in each case by the δ-electron density method.

Heavily ionizing h-tracks (group (1)) are ascribed to the fragmentation of the target nucleus, while the particles belonging to groups (2b), (3) and (4) are further on considered as fragments of the incident nuclei.

The single-charged relativistic particles consist of the particles produced during the interaction (mostly pions), relativistic recoil particles from the target nucleus and single-charged fragments of the incident nucleus. In this work it is assumed that all relativistic particles with emission angles $\theta \leq 3°$ ((2b)group) are due to single-charged fragments of the incident nucleus. This group of particles contains, however, some contamination due to π-mesons roughly estimated as 13%.

According to the above definition, in 734 events out of 852 analyzed inelastic collisions (i.e., ~90%) fragmentation of the incident ^{12}C nucleus occurs. It is worthwhile to mention that in the case of α-induced nuclear interactions the same criteria lead to a value of ~50% for the fraction of collisions accompanied by the fragmentation of the incident nucleus.

III. EXPERIMENTAL RESULTS

a). Multiplicity of secondary particles. Table II presents the average multiplicity values for secondary particles of different types in ^{12}C-A collisions at 50 GeV/c as well as the average multiplicities in ^{12}CA inter-

Table II

Average multiplicity / class of events	$\langle n_s \rangle$	$\langle n_g \rangle$	$\langle n_b \rangle$	$\langle n \rangle$ Z=1	$\langle n \rangle$ Z = 2
All events:	7.9 ± 0.3	6.1 ± 0.3	4.4 ± 0.2	1.18 ± 0.04	0.81 ± 0.03
$n_h \leq 6$	4.1 ± 0.2	1.0 ± 0.1	1.1 ± 0.1	1.28 ± 0.06	1.21 ± 0.04
$n_h > 6$	11.8 ± 0.4	11.4 ± 0.4	7.8 ± 0.2	1.07 ± 0.05	0.41 ± 0.03
$n_h \geq 28$	18.6 ± 0.7	22.3 ± 0.8	11.1 ± 0.5	0.56 ± 0.09	0.06 ± 0.02

actions for various groups of events, namely those with $N_h \leq 6$, $N_h > 6$ and $N_h > 28$. In table III a comparison of the average multiplicity values for p-A[6], d-A[2] and α-A[3] interactions is presented.

It should be kept in mind, however, that while the data for d, α and ^{12}C interactions were obtained in our experiments performed at the same momentum per incident nucleon, the data for p-nucleus interactions were obtained by an interpolation of data obtained for close but not the same energies of the primary; a compilation of these experimental data can be found in [7].

In Table IV the $n_h - n_s$ matrix is presented. The multiplicity distributions of h tracks for ^{12}CA collisions are shown in fig. 1 as well as the n_h -distributions for pA[6], dA[2] and αA[3] interactions.

The mean multiplicity of relativistic s-particles increases rapidly with increasing the mass number of the projectile nucleus (A_{proj}). The grey track multiplicity also increases with increasing $A_{proj.}$, while the multiplicity fragments of the target nucleus (b particles) decreases weakly with increasing of $A_{proj.}$

An analysis of the data from our present experiment and the data obtained in the works [2,3,6] leads to the conclusion that the n_s, n_g and n_b distributions significantly change with increasing $A_{proj.}$ value: the n_s distribution becomes broader (with no major change of its general shape), however; the n_g distribution for higher $A_{proj.}$ values contains an increased contribution of high n_g events; the n_b distribution for higher $A_{proj.}$ values contains an increased contribu-

Table III

	pA	dA	αA	^{12}CA
$\langle n_s^* \rangle$	1.6 ± 0.1	3.1 ± 0.1	4.4 ± 0.1	8.1 ± 0.3
$\langle n_g \rangle$	3.6 ± 0.1	2.3 ± 0.1	4.7 ± 0.2	6.I ± 0.3
$\langle n_b \rangle$	5.7 ± 0.2	5.3 ± 0.1	4.7 ± 0.2	4.4 ± 0.2

* In these average multiplicities the number of s-particles with $\theta < 3^{\circ}$ is included.

Table IV

Distribution $n_h - n_s$

n_h \ n_s	0	1	2	3	4	5	6	7	8	9	10	11	12	13	14	15	16	17	18	19	20	21	22	23	24	25	26	27	28	SUM
0	20	17	14	14	12	4	2			1																				84
1	32	22	17	8	9	4	2	1			1																			96
2	[illegible]	[illegible]	3	3	5	3	2	1	2	2	2	1																		39
3	[illegible]	[illegible]	9	7	3	2	4	4	[illegible]	2	2		1	2	3							1		1						58
4	4	[illegible]	7	5	[illegible]	4	3	1	5	2	1	4	2	1	1	2	1	1		1										63
5	3	7	3	5	[illegible]	3	1		1	4	1	3	1				1			1										41
6	1	4	6	3	2	3	3	2	4	4	3	4		4	2	3	1													51
7	3	6	4	1	4	1	3	2		1	1		3	2	1	1	2													35
8		2	6	4	1	6	5	1	2		1	1	2	2	1															34
9		2	6	2	3	1	4	3	2	4	1	1					1				1									31
10		1	3	1	5		1	1	3	2	3			1	1															22
11	1	1	1	2	[illegible]	3	2	2		2	1			1						1										20
12		1			2	1	1	2	1	1		1																		10
13				1	1	2	2	4	1	1	2		1			1	1													17
14			1				2				2	1		1	1	1				1	1									11
15						1			1					2							1									5
16				1			3			1	1			1	2	1	1		1		1									13
17			1		1	1	1	1		1	1		1			1					1					1				10
18					1	1				2			2	1	2	1			1							1				12
19			1	1		1	1			1	2		1			2														10
20							1	2				1	1		1			1		1			1							9
21				1						1	1			1	2	3	1			1	1			1	1		1		1	16
22				1	1	3						3		1	1			1												10
23						1	1		1					1	1		1		1	1		1								9
24					1		1						1	1		2		1		1		1						1		10
25								2	1			2	1						1	1					1					9
26									1	1	3	1					1			1	1					1				10
27				2				1					1	2	1			1		1	1		2							12
28														1	1	1		3			1		1		1					9
29								1		1	1	1	1		1			2	1	2										11
30								1		1	1				1	1	2		1	1	1							1		11
31													1					1	2	1			1					1	2	9
32										2				1			1							2						6
33									1								1		2			1		1					1	7
34							1																							1
35																					1		1			2				4
36													1	1		1			1		1	1					1	1		8
37															1			1	2			1								5
38															1					1				1				1		4
39																2					1									3
40								1								1									1					3
41															1			1	1											3
42																				1		1								2
43										1					1						1						1			4
SUM	78	84	86	60	75	44	45	33	28	38	31	24	21	27	27	24	16	13	14	17	14	7	6	6	4	5	3	5	4	839

In the distribution the following events are not included: n_s/n_h=10/44; 12/52; 13/50; 16/46; 17/45; 17/46; 19/45; 25/47; 29/27; 30/26; 30/33; 33/28; 35/31

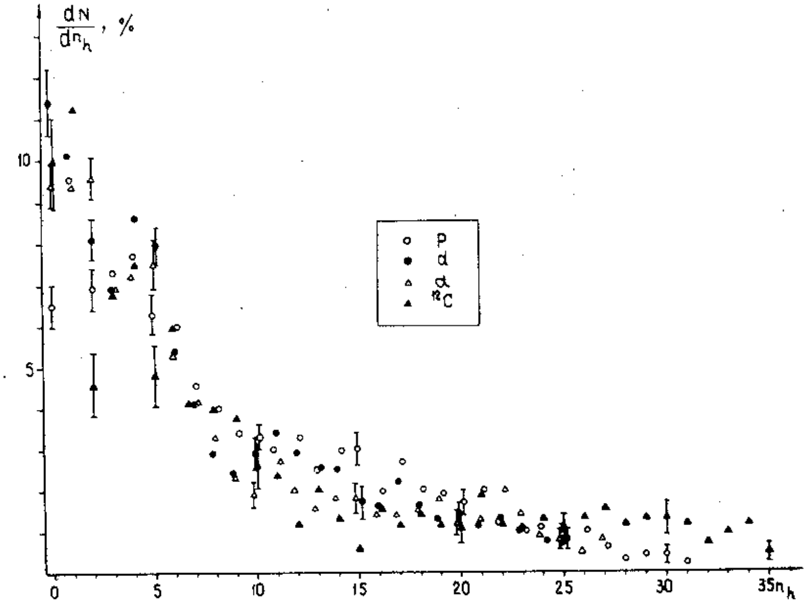

Fig. 1. The n_h distributions p-A, α-A and ^{12}C-A collisions.

tion of high n_g events; the n_b distribution for higher A_{proj} values contains an increased contribution of low multiplicity (n_b = 0,1) and very high multiplicity events.

An interesting conclusion can be derived from the analysis of the multiplicity dependence on the number (n_{int}) of primary nucleons which have interacted with the target nucleus. An estimation of this value can be obtained from the total charge (Q) of the observed secondary relativistic fragments which have not interacted, $Q = \Sigma n_i Z_i$, where n_i is the number of fragments with charge Z_i in any given star. The Q distributions is given in fig. 2. It can be seen that the distribution is almost uniform. The values of Q>6 appear

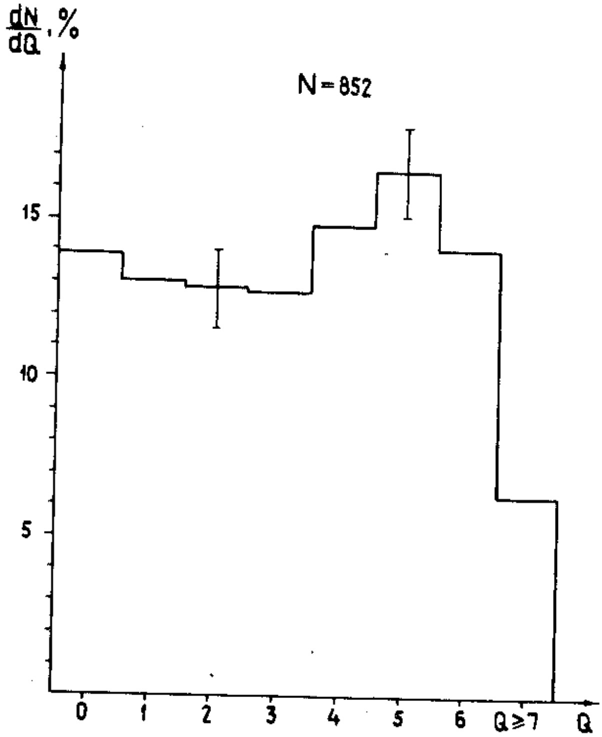

Fig. 2. The distribution of the total charge Q of the ^{12}C projectile fragments which have not interacted with the target nucleus.

in a small number of events due to uncertainties in the identification of single-charged fragments. The number of interacting nucleons of the projectile nucleus is on the average close to $n_{int} = 12-2.Q$, the value being slightly overestimated.

Figure 3 shows the dependence of the average multiplicity values of secondary particles on the value of n_{int} (and on Q). One can see that the multiplicity values increase rapidly with increasing n_{int} (or decreasing Q).

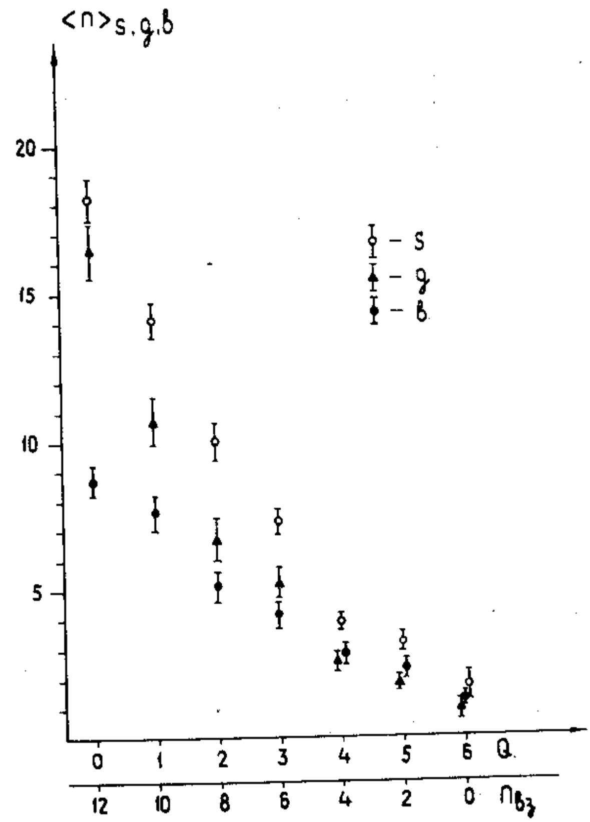

Fig. 3. The average multiplicity values of secondaries versus n_{int} and Q.

The value of n_{int} (or Q) seems to be a convenient experimental value, which can be used for classification of nucleus-nucleus interactions according to the degree of the "peripherality" of interactions. It seems reasonable to treat interactions with small Q (or large n_{int}) as "central" ones and those with large Q as "peripheral" ones, with a large value of the collision parameter.

b) Angular distributions. In fig. 4 the angular distributions of fragments of the incident nucleus in the region of small angles are compared with similar data for dA and αA collisions /2,3/.

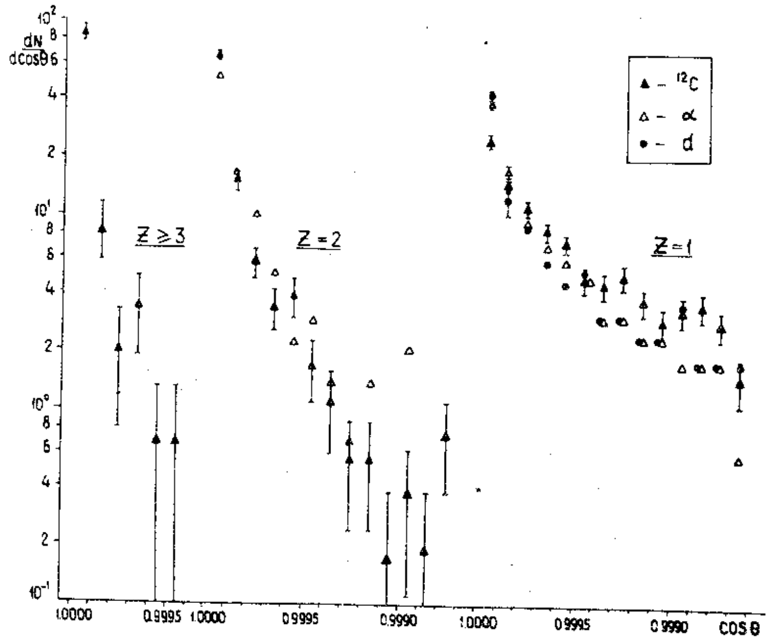

Fig. 4. The angular distributions of the projectile fragments of charge a) Z =1, b) Z =2 and c) Z ≥3 and analogous data for d-A and α-A collisions.

The angular distributions of single and double charged fragments are rather similar for ^{12}C-A and α-A interactions. The average values of emission angles for fragments decrease with increasing the fragment mass (the distributions are narrower). This fact was observed in many earlier works in which the fragmentation processes of relativistic nuclei have been studied.

The angular distributions of s, g and b particles for ^{12}CA interactions (not shown here) do not differ within experimental errors from those for collisions of lighter (p, d, α) projectile-nuclei.

Figures 5,6 represent the angular distributions of g and b particles in ^{12}CA events for various numbers of interacting nucleons in the projectile-nucleus (n_{int} or Q). The distribution shape is weakly dependent on n_{int}, while the dispersions of the angular spectra do not depend on n_{int} (or Q) within experimental errors.

The angular distributions do not show within statistical errors any structure which could be due to mechanisms of the shock wave type.

c) The $^{12}C \to 3\alpha$ dissociation. The dissociation reactions $^{12}C \to 3\alpha$, being of a particular interest, were studied separately. The events characterized by the presence of only 3 charged secondaries, each being emitted at an angle of $\theta \leq 3°$ and with charge Z = 2 (determined by δ-electron density method), were further considered as $^{12}C \to 3\alpha$ dissociation events.

20 events of such a type were selected out of 852 inelastic ^{12}C-A interactions, and additional 8 events were found in the course of further scanning. It is assumed that the momentum of each α-particle emitted from such dissociation events is equal to 1/3 of the momentum p_0 of the incident carbon nucleus. Consequently, the transverse momentum of each secondary α-particle equals

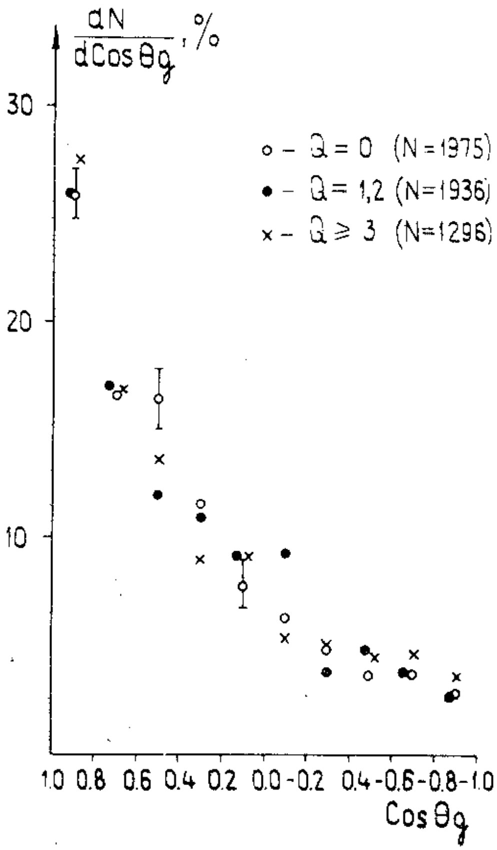

Fig. 5. The angular distributions of g-particles for the interactions with various values of n_{int}.

$p_{\perp i} = 1/3\, p_0 \cos\theta_i$.

The vector sum of $p_{\perp i}$ is equal to the transverse momentum transferred to the ^{12}C nucleus in the diffraction scattering process. Consequently, to a first approximation, the transverse momentum of an α-particle in the ^{12}C nucleus is equal to

$$\vec{p}^{\,*}_{\perp i} = \vec{p}_{\perp i} - \frac{1}{3}\sum_{i=1}^{3} \vec{p}_{\perp i},$$

and the distribution of $p^*_{\perp i}$ values is shown in fig. 7.

In 18 out of 28 analyzed events of the $^{12}C \to 3\alpha$ reaction the following structure was observed: two α-particles are emitted in a very narrow angular cone (with a very low relative $p_\perp$ momentum), while, probably, $p_\perp$ of the third α-particle compensates the sum of transverse momenta of the other two. This observation indicates that the diffraction dissociation $^{12}C \to 3\alpha$ is going in a cascade

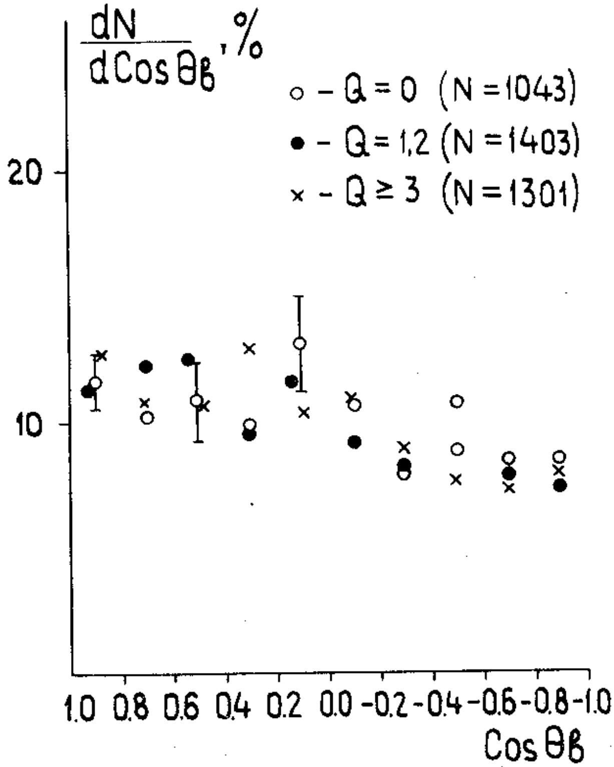

Fig. 6. The angular distributions of b-particles for the interactions with various values of n_{int}.

way, via an intermediate ^{8}Be state. It is known that a similar process was observed in the case of low energy photon interactions with ^{12}C nuclei.

IV. CONCLUSIONS

The results of this paper can be summarized as follows:

1. The average multiplicity values for secondary particles per interacting projec-

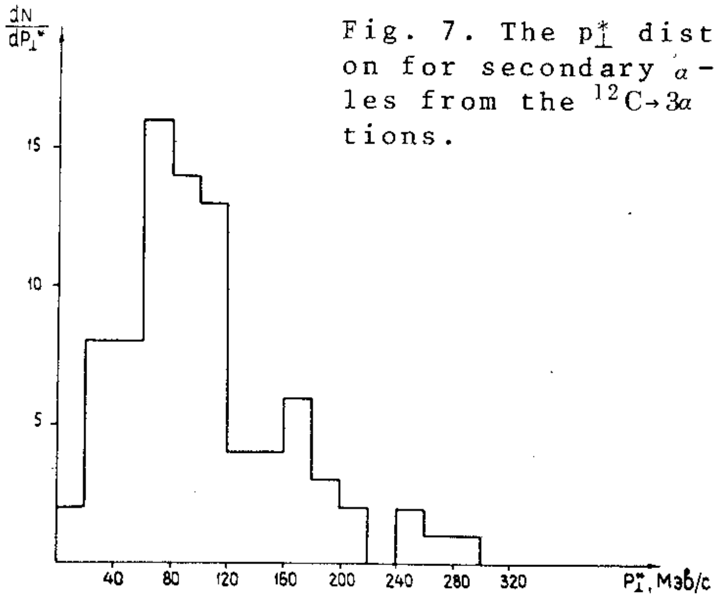

Fig. 7. The $p_{\perp}^{*}$ distribution for secondary α-particles from the $^{12}C \to 3\alpha$ reactions.

tile-nucleon are close for the interactions of d and α-particles and ^{12}C nuclei with emulsion nuclei.

2. It is found that charged fragments of the projectile-nucleus are observed in almost 90% of inelastic ^{12}CA interactions.

3. The dissociation process of the carbon nucleus into three α-particles has been observed. Its contribution is about 2.3% of the total number of inelastic interactions.

A more detailed investigation of ^{12}CA interactions is being carried out by Collaboration Laboratories, and results will be published elsewhere.

REFERENCES

1. A.M.Baldin. Invited Talk at the VI Intern. Conf. on High Energy Physics and Nuclear Structure, Los Alamos and Santa Fe, 1975; H.H.Heckman. Invited Talk at the V Intern. Conf. on High Energy Physics and Nuclear Structure, Uppsala, 1973; W.Greiner. Invited Talk at the 2-nd Heavy Ion Summer Study, Berkeley, 1974 (LBL-3675, 1975) p. 1.
2. BVDKLMT Collaboration. JINR, P1-6877, Dubna, 1972.
3. BVDKLMT Collaboration. JINR, P1-8313, Dubna, 1974.
4. B.Jykobson, P.Kullberg. Phys.Scripta, 13, 327, 1976.
5. R.Kaiser et al. Proc. 12-th Int. Cosmic Ray Conf., Denver, 1973. H.H.Heckman et al. Proc. 14-th Int. Cosmic Ray Conf., Munich, 1975.
6. H.Winzeler. Nucl.Phys., 69, 661 (1965).
7. V.S.Barashenkov, V.D.Toneev. Interactions of High Energy Particles with Nuclei, Moscow, Atomizdat, 1972.

Received by Publishing Department on July 11, 1977.

SUBJECT CATEGORIES
OF THE JINR PUBLICATIONS

Index	Subject
1.	High energy experimental physics
2.	High energy theoretical physics
3.	Low energy experimental physics
4.	Low energy theoretical physics
5.	Mathematics
6.	Nuclear spectroscopy and radiochemistry
7.	Heavy ion physics
8.	Cryogenics
9.	Accelerators
10.	Automatization of data processing
11.	Computing mathematics and technique
12.	Chemistry
13.	Experimental techniques and methods
14.	Solid state physics. Liquids
15.	Experimental physics of nuclear reactions at low energies
16.	Health physics. Shieldings
17.	Theory of condensed matter

Издательский отдел Объединенного института ядерных исследований.
Заказ 23599. Тираж 670. Уч.-изд. листов 0,85.
Редактор Э.В. Ивашкевич. Подписано к печати 5.09.77 г.
Корректор Р.Д. Фомина.